 doi:10.20944/preprints202111.0411.v1

Article

Preparation and physicochemical properties of modified corn starch – chitosan biodegradable films

Enrique Javier Jiménez-Regalado [1], Carolina Caicedo [2], Abril Fonseca-García [1,3], Claudia Cecilia Rivera-Vallejo [1], and Rocio Yaneli Aguirre-Loredo [1,3]*

[1] Centro de Investigación en Química Aplicada (CIQA), Blvd. Enrique Reyna Hermosillo 140, Saltillo, Coahuila 25294, México; enrique.jimenez@ciqa.edu.mx (E.J.J.-R.), claudia.rivera@ciqa.edu.mx (C.C.R.-V.), abril.fonseca@ciqa.edu.mx (A.F.-G.), yaneli.aguirre@ciqa.edu.mx (R.Y.A.-L.)
[2] Grupo de Investigación en Química y Biotecnología (QUIBIO), Facultad de Ciencias Básicas, Universidad Santiago de Cali, Pampalinda, Santiago de Cali 760035, Colombia; carolina.caicedo03@usc.edu.co (C.C.)
[3] CONACYT - CIQA, Blvd. Enrique Reyna Hermosillo 140, Saltillo, Coahuila 25294, México
* Correspondence: yaneli.aguirre@ciqa.edu.mx (R.Y.A.-L.)

Abstract: Starch is a biopolymer with wide potential for the generation of new biodegradable packages due to its high availability and low price. However, due to its weak functional properties, it is necessary to limit the interaction of some hydroxyl, and to evaluate blends with other polymers to improve their performance. Glycerol plasticized acetylated corn starch films were developed by the casting method, and the impact of incorporating chitosan (TPS:CH) at various proportions (75:25, 50:50, and 25:75 v/v) was studied. The effect of the chitosan ratios on the films' physical, mechanical, water vapor barrier, and thermal properties was evaluated. Chitosan protonated amino groups promote the formation of intermolecular bonds, improving the tensile strength, the thermal stability, the water adsorption capacity, and the gas barrier of starch films. Where the film composed of TPS25-CH75 was the one that presented the best barrier to water vapor. These composite films are a good option for development of biodegradable packaging.

Keywords: Biodegradable film; thermoplastic starch; chitosan; mechanical properties; water vapor permeability

1. Introduction

It is well known worldwide that humanity is going through a critical pollution problem. One of the most discarded materials is plastic, mainly the one used in the food industry. These plastics are used for the packaging, conservation, transport, and consumption of food products. Because of this, several investigations have been proposed to develop more environmentally friendly materials that can replace conventional synthetic plastics. These new materials can be obtained from various mixtures of biodegradable polymers combined with some additives such as plasticizers, antioxidants, and antimicrobials.

Starch is a natural polymer, which due to its high availability in nature and affordable price, can be an attractive option for biodegradable packaging. Starch is composed of two molecules, amylose, and amylopectin. Amylose is a linear polysaccharide of α-1,4 linked D-glucopyranose, while amylopectin is a highly branched molecule consisting of chains of α-D-glucopyranosyl residues linked by 1,4 and 1,6 bonds. Due to its wide availability in nature, starch is an excellent choice for the manufacture of low-cost, biodegradable packaging materials. However, starch-based materials are brittle and susceptible to moisture, which is why research has been developed to improve their functional performance. Starch can be modified in various ways to change its processing properties as well as the materials generated. One way of modification is through chemical processes such as esterification and acetylation. Acetylated starch contains acetyl groups that have replaced some of the OH groups in anhydroglucose. These acetyl groups break the inter-

Preprints (www.preprints.org) | NOT PEER-REVIEWED | Posted: 23 November 2021 doi:10.20944/preprints202111.0411.v1

and intramolecular bonds of the starch, weakening its structure allowing higher mobility of the polymeric chains of the amorphous region [1, 2]. Acetylated starch has a lower gelatinization temperature than regular starch, as well as a slower retrograde rate [1]. The films obtained with these modified starches show higher elongation and lower water vapor permeability than films based on native starch [3]. Biodegradable starch films usually have good mechanical strength; however, their deficiency lies in the high permeability to gases, such as water vapor. Another way to modify the functional properties of starch-based materials is to blend them with other polymers or additives. Starch has been mixed with some other biopolymers such as polyvinyl alcohol and chitosan, to improve its physicochemical and functional properties [1, 4, 5].

Chitosan is a natural linear polysaccharide derived from chitin extracted from the exoskeleton of crustaceans, a by-product of the waste from the fishing industry [2]. Due to its cationic nature having important functional qualities, it is biodegradable, non-toxic, biofunctional, biocompatible, with antimicrobial and antifungal activity [6]. Several studies have developed mixtures of starches with chitosan, finding that they can generate films with good handling, where the mechanical and barrier performance depends significantly on the concentration of chitosan added to the starch, as well as its deacetylation degree [7, 8].

The objective of this study was to evaluate the influence of acetylated corn starch-chitosan (TPS:CH) at three ratios (75:25, 50:50, and 25:75 v/v) on the mechanical, gas barrier, thermal, and water vapor sorption properties of a biodegradable film based on modified (acetylated) starch films plasticized with glycerol.

2. Materials and Methods

2.1. Materials

The biodegradable polymers used were modified food starch (Pure-Gel, B994) obtained from Grain Processing Corporation (Muscatine, Iowa, U.S.A.), and chitosan (90% deacetylation degree) from Alfadelta Materias Primas (Mexico). Anhydrous glycerol from J.T. Baker (Mexico) as a plasticizer. The glacial acetic acid acquired from Productos Quimicos Monterrey (Mexico). LiCl, CH_3COOK, $MgCl_2$, K_2CO_3, NaBr, NaCl, KCl, and $BaCl_2$ (Jalmek Cientifica, Mexico) to prepare supersaturated saline solutions to obtain environments with equilibrium relative humidity (RH) of 11, 22, 32, 43, 57, 75, 84, and 90%, respectively.

2.2. Preparation of films

To prepare the film-forming solutions five starch:chitosan (TPS:CH) ratios were developed 0:100, 75:25, 50:50, 25:75, and 0:00, labeled as TPS100-CH0, TPS75-CH25, TPS50-CH50, TPS25-CH75, and TPS0-CH100, respectively. The corresponding amount of starch (to prepare it at 6% w/v) was dispersed in distilled water, and the plasticizer was added at a concentration of 30% (w/w of total polymers) when the starch dispersion reached 50 °C, a correspondent volume (mL) of a 1% (w/v) solution of chitosan (dissolved in 1% v/v acetic acid solution) was added. The filmogenic solutions were kept under constant stirring, and the temperature was increased to 90-92 °C and kept for 7 min for the gelatinization of the starch. 100 mL of filmogenic solution was poured into 150 x 150 mm acrylic molds and dried at 65 °C for 5 h in an oven (Oven Series 9000, Thermolyne). The dried films were peeled and kept for 48 h at room temperature (~25 °C) and at a 54% RH, in desiccators containing a supersaturated solution of NaBr prior to evaluating the functional properties.

2.3. Thickness

The film thickness was measured in ten random positions on the entire surface of the material using a digital micrometer (Mitutoyo, model C112EXB, USA, precision 0.001 mm). The average and standard deviation of ten film samples were obtained.

Preprints (www.preprints.org) | NOT PEER-REVIEWED | Posted: 23 November 2021 doi:10.20944/preprints202111.0411.v1

2.4. Water solubility

The capacity and resistance to being in contact with the liquid water of the materials were determined with the solubilization capacity in water at room temperature (25 °C), following the [9] methodology.

2.5. Fourier Transform Infrared (FT-IR) analysis

The chemical structure of films was analyzed by Fourier Transform Infrared (FT-IR) using a NICOLET iS10 spectrometer of Thermo Fisher SCIENTIFIC (Madison Wisconsin, USA). The measurements were done by Attenuated Total Reflection (ATR).

2.6. X-ray diffraction (XRD) analysis

Following the methodology proposed by Fonseca-García, Jiménez-Regalado [9] and using a Siemens D500 powder diffractometer, the arrangement of the structural matrix of the films was determined.

2.7. Thermal properties

The thermal behavior of the materials was determined through the Differential scanning calorimetry (DSC) and Termogravimetrical analysis (TGA) techniques, employing the DSC 2500 Discovery (TA Instruments, USA) and TGA Q500 (TA Instruments, USA) analyzer equipment, and following the methodology proposed by Fonseca-García, Jiménez-Regalado [9].

2.8. Adsorption isotherms

To determine the resistance of materials to humidity present in the environment and to evaluate how much water they can absorb, each material's water vapor adsorption isotherm was determined, using the static microclimate method, following the methodology developed by the COST90bis Project [10] and by Aguirre-Loredo, Rodríguez-Hernández [11] with some modifications. The film samples (4 cm^2) were placed in airtight plastic containers with supersaturated saline solutions, generating an 11-90% RH range. The containers were stored at room temperature (25 °C) for 14 days. The GAB mathematical model (Eq. 1) was used to describe the sorption isotherms of the films with different starch-chitosan ratios.

$$X = \frac{X_m C K a_w}{(1-K a_w)(1-K a_w+C K a_w)} \quad (1)$$

Where the parameters *Xm* is the moisture content in the monolayer, *C* is the constant related to the sorption in the first layer, *K* is a constant related to the sorption of water molecules in multilayer.

2.9. Mechanical properties

The mechanical properties of 10 film samples of 10 mm x 50 mm were measured using a texture analyzer TA.XT Express Enhanced texture analyzer (Stable Micro Systems, England), equipped with tension grips (A/TG) at room temperature (25 °C), operating at a cross-head speed of 1 $mm.s^{-1}$, with an initial separation of 25 mm, according to the D882-12 standard [12]. The tensile strength (TS) and the percentage of elongation at break (%E) were calculated.

2.10. Water vapor permeability (WVP)

The water vapor permeability was determined according to the methodology proposed by Aguirre-Loredo, Rodríguez-Hernández [11] following the ASTM E96-02 [13] standard. The permeability cell consisted of a glass container with an internal diameter of 24.64 mm, in its interior, silica gel was placed (~0% RH). Film discs were mounted on

Preprints (www.preprints.org) | NOT PEER-REVIEWED | Posted: 23 November 2021 doi:10.20944/preprints202111.0411.v1

permeation cell; the covered cell was placed in a desiccator containing a supersaturated saline solution of $BaCl_2$ (90% RH) generating a water vapor differential pressure of 2854.23 Pa. The cell was weighed seven times at 60 min intervals. The determinations were made in triplicate.

2.11. Statistical analysis

The results were analyzed for statistical significance by analysis of variance (ANOVA) and Tukey's test with a $p<0.05$ significance level using the OriginPro 8.5.0 SR1 software (OriginLab Corporation, Northampton, Massachusetts, USA).

3. Results and Discussion

3.1. Thickness and solubility

A significant difference was observed in the thickness of the polymeric materials (Table 1) as a function of the proportion of biopolymers; however, this result is to be expected because the initial concentration of each of the original polymeric solutions is different, remembering that the starch is found at a concentration of 5%, while chitosan is at 1%. However, this behavior of thickness as a function of mass did not appear as expected. The formulations that followed the expected behavior contained pure chitosan (TPS0-CH100, smallest mass), which presented the smallest thickness, and the formulation based on starch-chitosan in a TPS75-CH25 ratio (higher mass of biopolymers).

Table 1. Thickness, water solubility, and water vapor permeability of thermoplastic modified cornstarch and chitosan composite film.

Starch:chitosan volume solution ratios	Thickness (μm)	Solubility (%)	WVP $x10^{-11}$ ($g.m^{-1}.s^{-1}.Pa^{-1}$)
TPS100-CH0	110.36 ± 1.61 ^{d}	30.70 ± 2.35 ^{a}	26.20 ± 6.43 ^{e}
TPS75-CH25	162.54 ± 7.84 ^{e}	47.24 ± 2.07 ^{b}	4.95 ± 0.81 ^{c}
TPS50-CH50	70.06 ± 0.95 ^{b}	49.86 ± 5.30 ^{b}	5.74 ± 0.77 ^{d}
TPS25-CH75	90.46 ± 6.48 ^{c}	70.92 ± 7.42 ^{c}	0.55 ± 0.03 ^{a}
TPS0-CH100	49.07 ± 2.59 ^{a}	68.84 ± 6.68 ^{c}	4.01 ± 0.52 ^{b}

Values with a different letter in the same column denote significant difference (Tukey test; $p<0.05$). Values are given as mean ± standard deviation ($n = 10$ for thickness and $n = 3$ for solubility and WVP).

One of the factors that most affect and concern when designing and using a completely biodegradable material is the susceptibility or damage of the material due to contact with water since most biopolymers are hydrophilic. The biodegradable films made in this study showed increased solubilization capacity in liquid water, as observed in the values shown in Table 1. The solubility in water of pure starch films is similar to that reported by Colussi, Pinto [3] in acetylated starch; and higher than native corn starch [9]. This higher solubility of acetylated films compared to those made from native starch is due to the ease of incursion of water molecules into the structural matrix of the modified starch film, as a consequence of lower retrogradation. The solubility of the composite materials increased significantly with the increase in the proportion of chitosan present in the composite films. The thickness is a parameter that can also influence the solubility of the materials since although the material may have a hydrophilic nature, the higher the thickness, the resistance to dissolution will be slightly higher. According to the data in

 doi:10.20944/preprints202111.0411.v1

Table 1, the solubility was higher in the materials with the smallest thickness and the highest chitosan ratio, which is correlated.

3.2. Fourier Transform Infrared (FT-IR) analysis

Figure 1 shows the spectra of blends of biodegradable films. The acetylated TPS showed characteristic bands detailed below: at 3282 cm^{-1} the stretching of O-H, which decreases its absorption with increasing chitosan concentration. This absorption band is strong and broad, and it overlaps with -NH stretching vibration and intermolecular hydrogen bonds in the mixtures (TPS75-CH25, TPS50-CH50, and TPS25-CH75). At a wavenumber of 2924 and 2887 cm^{-1}, symmetric and asymmetric stretching vibrations of methyl groups CH_2 are observed in the spectrum of thermoplastic starch [14]. At 1646 cm^{-1} bending vibration of OH (water), and carbonyl appears in chitosan at the same wavenumber. CH and CH_2 deformations are evident at 1412 cm^{-1}. In the region of 1242 and 1240 cm^{-1}, O-H vibrations (bending) and C-O stretching of the acetate are present. Some bands were also observed that could be attributed to the formation of hydrophilic colloids in the composite films at 1077 cm^{-1}, 1018 cm^{-1}, and 927 cm^{-1} (C-O stretching and O-H bending), 851 cm^{-1} (H-atoms), 651 cm^{-1}, and 600 cm^{-1} (plane bending) [15]. While in the region comprising 997-706 cm^{-1} it is related to vibratory modes of the d-glucopyranosyl ring as well as to the skeletal modes of the pyranose ring [7]. Likewise, chitosan (CH) exhibits a series of bands at 898, 1034, and 1088 cm^{-1} corresponding to stretching vibrations of the C–O group, and at 1153 cm^{-1} corresponding to the asymmetric stretching of C–O–C bridge, also related with the saccharide structure [16]. Typical vibration bands for amide I and II were observed at 1646 cm^{-1} for C=O stretch, 1554 cm^{-1} for flexion -NH_2, and 1378 cm^{-1} flexion -CH_2. The absorption band at 3409 cm^{-1} (strong and broad) was attributed to the stretching vibration of –OH, the stretching vibration of –NH, and the intermolecular hydrogen bonds of other polysaccharides. Figure 2 shows the possible intra- and inter-molecular interactions between the different components of biodegradable blends.

Regarding the starch bands not discussed in the region 1200 to 900 cm^{-1}, it could be inferred that this analysis is sensitive to changes in the structure at the molecular level of starch. In general, these bands exhibited a broadening due to the multiple and stronger intermolecular interactions that influence the vibration of the C-O group. Differences between the 1047 cm^{-1} bands of the crystalline regions and 1022 cm^{-1} of the amorphous region were observed between the complexes [17]. Likewise, the absorption intensity of the band at 995 cm^{-1} related to the double helices of the amorphous region, allowed estimating the degrees of order (DO, $R_{1047/1022}$) and double helices (DD, $R_{995/1022}$) in the mixtures (Figure 1b) [18]. In general, a linear trend is observed for DO that increases proportionally with increasing chitosan content. However, the TPS50-CH50 sample reflects a discontinuity with values higher than those corresponding to this trend. The increased DO reflects stronger intermolecular interactions between TPS and low chitosan contents (~25%). On the other hand, the DD values show a rational trend where the values decrease proportionally with the increase in chitosan. In particular, TPS50-CH50 shows values that are equal to TPS75-CH25; it is believed that double helix destructuring was limited in that formulation. This can be explained due to the fact that interaction competition with the plasticizer is generated in the presence of a higher content of chitosan. An increase in structural ordering was observed in the amorphous region promoted by the increase in chitosan content. However, there was also a lower intramolecular interaction (H-bonds) that reflects the decrease in double helices.

Preprints (www.preprints.org) | NOT PEER-REVIEWED | Posted: 23 November 2021 doi:10.20944/preprints202111.0411.v1

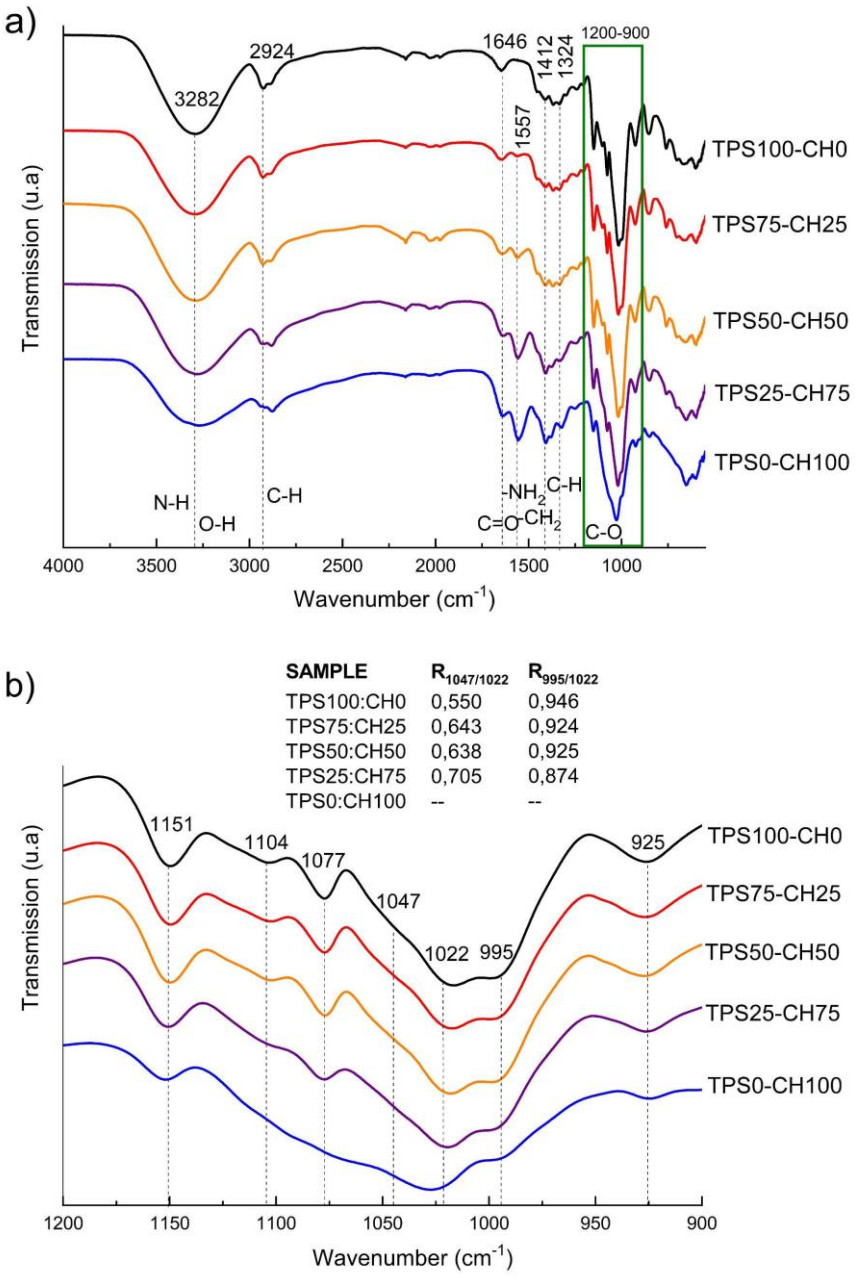

Figure 1. a) ATR- FTIR spectra of starch-chitosan films. b) amplified region between 1200 cm^{-1} to 900 cm^{-1}, this relates the values of $R_{1047/1022}$ and $R_{995/1022}$ of starch films-chitosan.

Preprints (www.preprints.org) | NOT PEER-REVIEWED | Posted: 23 November 2021 doi:10.20944/preprints202111.0411.v1

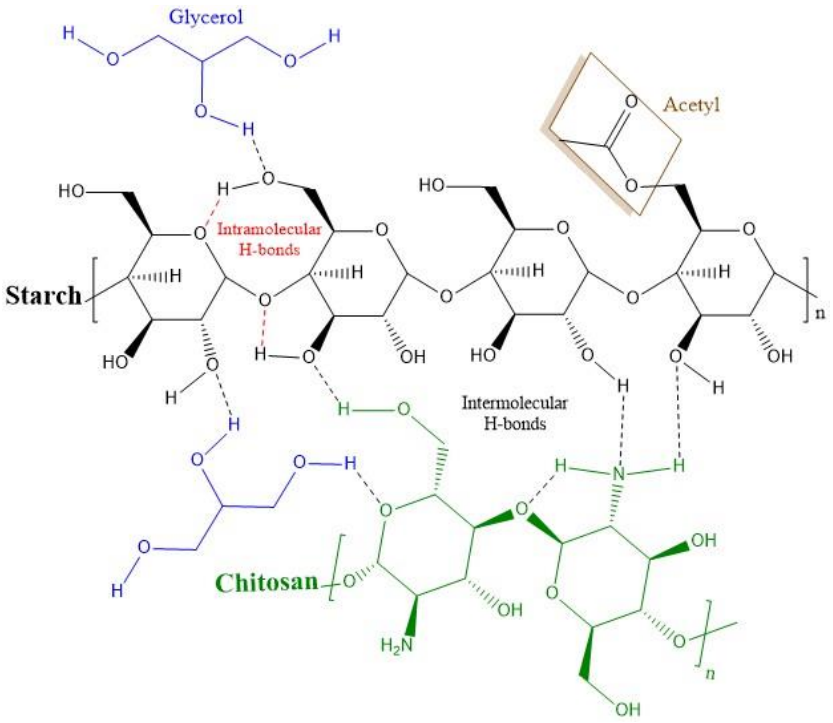

Figure 2. Proposed molecular interactions between starch, chitosan and glycerol.

3.3. X-Ray diffraction

Figure 3 shows the diffractograms of blends of biodegradable films, in the starch film, are identified peaks at 2θ = 12.5°, 15°, 17.5°, 20°, and 22.5°, while chitosan film showed diffraction peaks at 2θ = 13°, 15°, 20°, and 22.5°. In spite of the biopolymer precursor of the blend films showing crystallinity, the blend TPS75-CH25, TPS50-CH50, and TPS25-CH75 showed to be amorphous, this result indicates that chitosan avoids the retrogradation of starch.

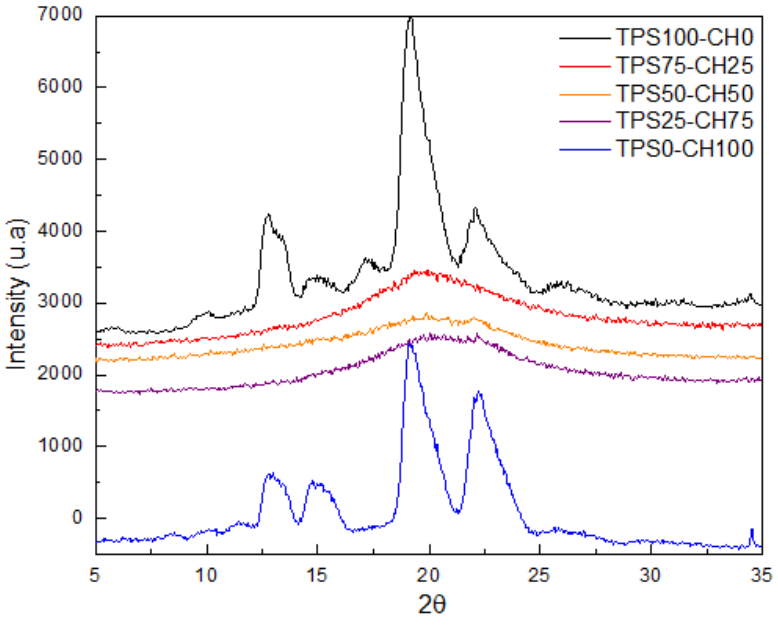

Figure 3. XRD diffractograms of starch:chitosan (TPS:CH) films.

Preprints (www.preprints.org) | NOT PEER-REVIEWED | Posted: 23 November 2021 doi:10.20944/preprints202111.0411.v1

However, chitosan film indicates that the heat treatment evaporates the solvent of films to help reorganize the crystalline structure, due to chitosan has three typical planes 1 1 0, 0 2 0, and 1 2 0, however, the chitosan films showed another peak, which it is associated with peak 1 0 1. Also, these peaks are shifted to lower angles, this result indicates an expansion of the crystal lattice of chitosan and is reported by Fan, Hu [19]. In relation to acetylated starch the diffractogram showed short and wide peaks, these peaks are indicative of ordering in the polymeric matrix, however, the peak at 2θ = 20° is characteristic of an acetylated starch, so that, this peak demonstrates the successful acetylation of this starch, Also. The wide peaks corroborated disorder in the crystalline structure of starch that could be attributed to the amylose and the amylopectin double helices of starch were ruptured after the substitution of the hydroxyl groups by bulkier acetyl groups [20, 21].

3.4. Thermal properties

It is observed that the thermal stability (Figure 4 and Table 2) of plasticized modified starch film (TPS100-CH0) is higher than that of chitosan film (TPS0-CH100). In both cases, there are three thermal events related to weight loss: the first is below 150 °C, where the TPS100-CH00 loses 8%, while the TPS0-CH100 at this same temperature has lost 20%. The second event occurs below 300 °C where the TPS100-CH00 loses 42%, while the TPS0-CH100 at this same temperature has lost 60%.

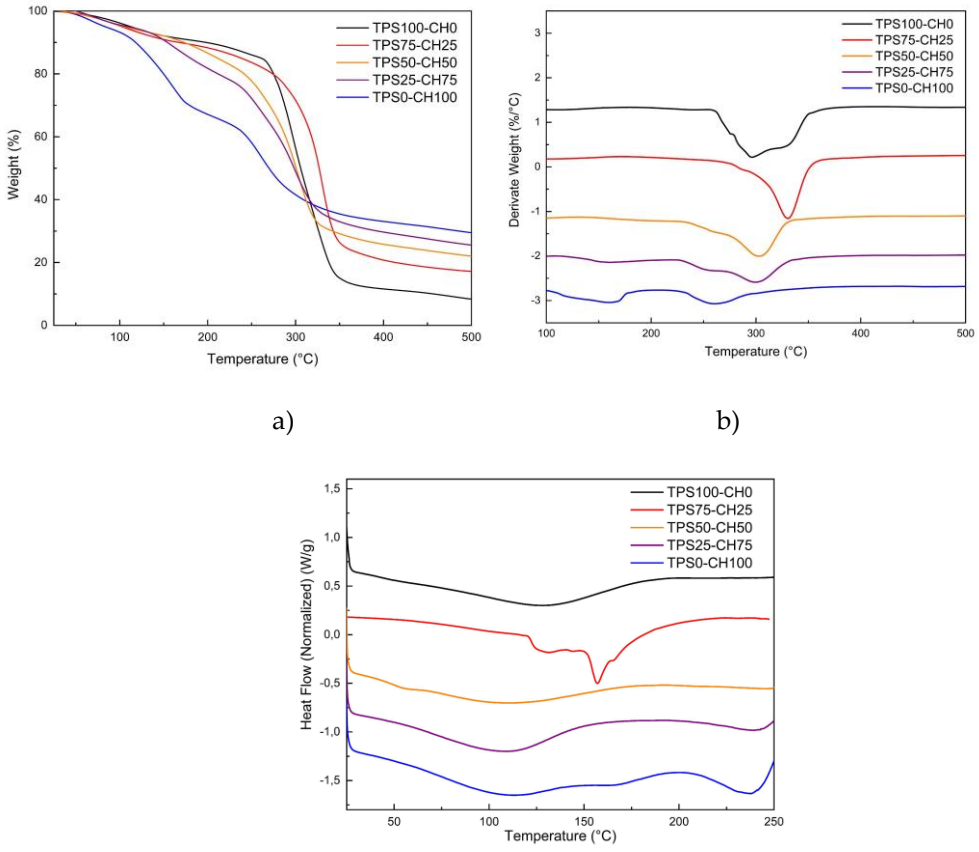

a) b)

c)

Figure 4. Thermal behavior of starch:chitosan films: a) TGA, b) DTG and c) DSC.

Preprints (www.preprints.org) | NOT PEER-REVIEWED | Posted: 23 November 2021 doi:10.20944/preprints202111.0411.v1

For the case of the TPS50-CH50 and TPS25-CH75 blends, they present intermediate values to the controls. Likewise, the decomposition of chitosan into amino units (and deacetylation is complete) occurs, the glycerol evaporates (at 290 °C, approximately) and the cleavage of the polymeric starch chains begins. The last event occurs after 300 °C, where the decomposition product residues are evident (of the -CHOH group and starch cyclic structures arise). The best thermal performance was presented by the TPS75-CH25 blend, which manages to increase the value of the maximum degradation temperature by 11.4% with respect to TPS100-CH0.

Table 2. Weight losses of 10% (T_{10}), weight losses of 30% (T_{30}), maximum degradation (T_{d1}), maximum degradation (T_{d2}), glass transition (T_g), and melting (T_m) temperatures, results based on the obtained TGA and DSC thermograms for the starch-chitosan (TPS-CH) biodegradable films.

Film sample Starch-chitosan (TPS-CH) ratios	T_{10}	T_{30}	T_{d1*}	T_{d2*}	T_{g1*}	T_{m1}	T_{g2*}
	°C						
TPS100-CH0	198.3	287.7	--	295.9	55.1	127.6	
TPS75-CH25	168.0	303.0	287.3	330.7	--	131.4	156.6
TPS50-CH50	173.2	270.3	261.1	303.1	56.2	111.1**	111.1**
TPS25-CH75	158.3	256.0	261.0	300.0	--	108.9**	108.9**
TPS0-CH100	118.1	179.4	259.7	--	--		163.8

*Temperatures: subscript 1 related to chitosan and 2 related to starch.

** Widening by overlapping bands of transitions: T_m and T_{d2}.

The thermal transitions (Figure 4) for the different samples present first and second-order transitions that relate the gelatinization temperature around 57 °C for starch and between 110 °C and 125 °C the melting temperature of thermoplastic starch, a product of plasticization. For chitosan, the glass transition temperature is observed around 112 °C, this value coincides with that reported by other authors [22], which discusses that in addition to plasticizer content, variability in crystallinity may be due to factors such as water content, degree of deacetylation, hydroxyl, and amino groups available. In this way, the T_{g2} of the mixtures decreases due to the plasticizer content and in the presence of low starch contents, which mobilize the chitosan chains through the protonation of the amino group (H-bond), according to the free volume theory [23]. The TPS75-CH25 sample shows a higher restriction in molecular mobility showing a higher and more defined Tm with respect to TPS100-CH00. This effect is consistent with the strong interactions reported in the FT-IR analysis and also with the DO. Modification by acetylation of starch causes its partial molecular hydrolysis, reducing the length of the glucose chains. Therefore,

Preprints (www.preprints.org) | NOT PEER-REVIEWED | Posted: 23 November 2021 doi:10.20944/preprints202111.0411.v1

modified starch films have a lower decomposition temperature than those based on native starch [3].

3.5. Water vapor adsorption isotherms

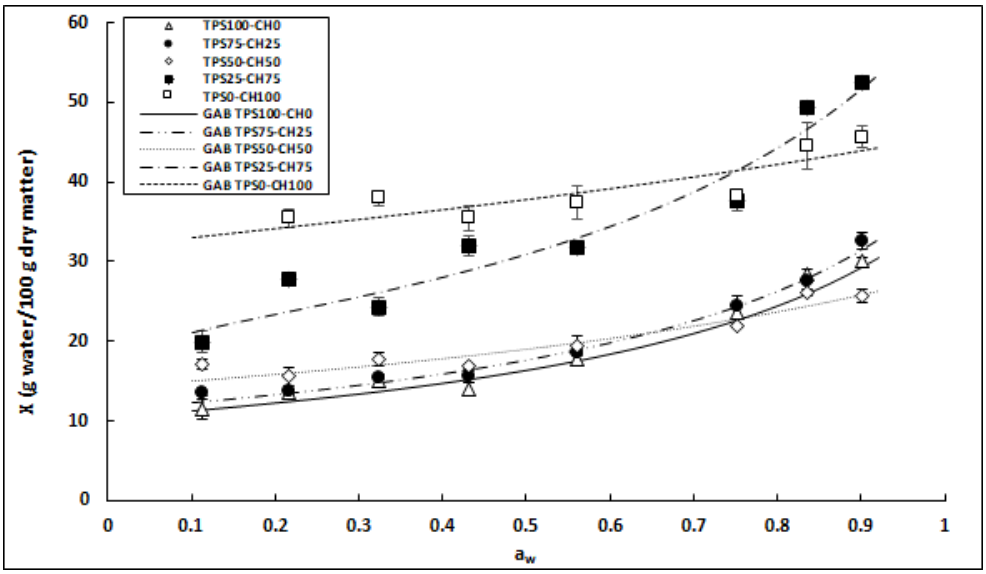

Figure 5. Moisture adsorption isotherms of starch:chitosan films at 25 °C, experimental data (symbols) and fitted to the GAB model (lines).

The water vapor adsorption behavior of the materials is an important parameter that needs to be evaluated when it is desired to use it as a packaging film. The moisture that these packages can adsorb when exposed to certain environmental conditions is a factor that influences and can modify the mechanical and gas barrier properties. Figure 5 shows the experimental and fitted moisture adsorption isotherms of TPS:CH films at 25 °C. It was observed that the water vapor adsorption of the films increased as a function of the content of chitosan present in the formulation. Films of pure starch (white triangle symbol) had the lowest moisture absorption throughout the relative humidity (RH) range, with maximum absorption of 30% when exposed to 90% RH, while the pure chitosan films (white box symbol) absorbed up to 46% moisture at the same RH. TPS:CH composite films exhibited intermediate adsorption behavior than pure films; this behavior occurred in environments of a_w < 0.8 (Figure 5). Above 0.8 a_w, there was no relationship with the proportion of biopolymers, mainly in the TPS25-CH75 composite films (black box symbol). Likewise, it has been reported that the water adsorption behavior of biopolymers such as starch may be a function of the composition and source of extraction [24]. Some studies have reported that the gas permeability of these materials is highly dependent on their water content [11]. A high water content increases the molecular mobility of the polymer matrix, affecting the diffusion of gas molecules and increasing their permeation; contrary result to that observed in this study. The pure starch film (TPS100-CH0) was the one that presented the highest WVP (Table 1) and the least water absorption (Figure 5), contrary to that presented by both the pure chitosan film (TPS0-CH100) and the TPS25-CH75 composite film. Qiao, Ma [25] reported a similar result in chitosan films.

The water vapor adsorption experimental data were fitted to the isothermal model of Guggenheim-Anderson-de Boer (GAB). The GAB model parameters (Xm, C, k) and the correlation coefficients (R^2) for each biodegradable TPS:CH composite film is shown in Table 3. The model obtained an adjustment value R^2>0.9, being an indication that this mathematical model is adequate to describe the values and the phenomenon of water

Preprints (www.preprints.org) | NOT PEER-REVIEWED | Posted: 23 November 2021 doi:10.20944/preprints202111.0411.v1

vapor adsorption observed in the evaluated materials. The parameter *Xm* corresponds to the moisture content present as the first layer of water, which interacts directly with the material, also called monolayer, and is the optimal water content for the conservation and storage of dry products. An increase in the amount of water present in the monolayer of the material was observed as the chitosan ratio increased in the starch films (Table 3). The acetylation degree (AD) has a significant influence on the first stage of adsorption of water vapor in chitosan. In chitosan with a low degree of acetylation, the number of available sites is low, so that any form of water vapor is easily adsorbed [26].

Table 3. GAB model parameters and regression coefficient R^2 calculated for biodegradable starch:chitosan films.

Starch-chitosan volume solution ratios (TPS-CH)	X_m	C	k	R^2
TPS100-CH0	10.71	1540.74	0.72	0.989
TPS75-CH25	11.35	9510.04	0.71	0.994
TPS50-CH50	14.38	15718.83	0.49	0.975
TPS25-CH75	20.85	241.73	0.66	0.963
TPS0-CH100	32.20	4555.95	0.29	0.919

3.6. Mechanical properties

The behavior of the mechanical properties of the tensile strength (TS) and the percentage of elongation at break (%E) of starch-chitosan biodegradable films with three biopolymer ratios (75:25, 50:50, and 25:75) and the pure films (starch, and chitosan) are presented in Figure 6. In the first instance, the ductility of the modified starch film (TPS100-CH0) and the stiffness of the chitosan films (TPS0-CH100) are observed. An increasing trend is observed in the TS values (Figure 6a) with increasing chitosan content. However, the TPS25-CH75 ratio remains unchanged at 8.04 MPa compared to the TPS50-CH50 ratio. On the other hand, the %E values (Figure 6b) decrease dramatically when incorporating high contents of chitosan (>50%). The differences in the results between the biopolymeric mixtures can be associated with the distribution and density of the molecular interactions that orient the functional groups of each polymer [27]. Several studies have shown that the tensile strength of starch films is higher with the increase in the concentration of chitosan [7]. This phenomenon is due to the interactions between the amino groups (NH_2) of chitosan and OH- from starch, which promotes the formation of intermolecular bonds, improving the tensile strength behavior of materials. It has been reported that the improvement of the mechanical behavior of the starch films with the incorporation of chitosan is observed when the concentration of chitosan is at least 40% [7]. The values of mechanical properties of tensile stress and elongation at fracture of the films made with the polymers pure (TPS100-CH0 and TPS0-CH100) are similar to those reported by other authors of pure films of the same biopolymers [28].

Preprints (www.preprints.org) | NOT PEER-REVIEWED | Posted: 23 November 2021 doi:10.20944/preprints202111.0411.v1

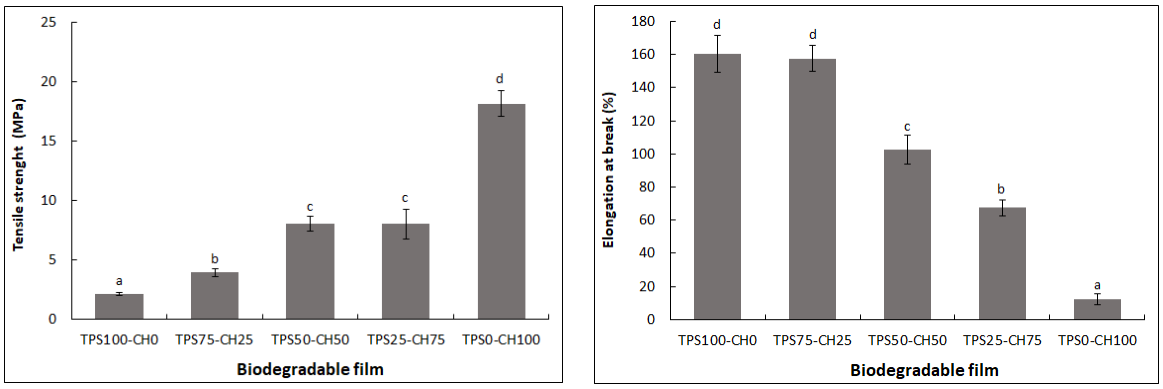

(**a**) (**b**)

Figure 6. Mechanical properties of starch:chitosan biodegradable films. (**a**) Tensile strength; (**b**) Elongation at break expressed as percentage.

In general, the "rule of mixtures" is not fulfilled according to the results found in this study, despite incorporating a constant plasticizer content on the total base of the polymers, it is observed that it does not exert a compatibilizing effect or homogeneous interaction with each polymer. Consequently, the interactions are stronger between glycerol and starch with respect to glycerol and chitosan, this behavior is evidenced with the TS value of sample TPS75-CH25, this increased by 84.6%, maintaining ductility (elongation ~160%) with respect to the starch control (TPS100-CH0). Other authors have discussed the effect of adding different proportions of glycerol on starch:chitosan=6:4 (w/w) on the mechanical properties. Higher content of plasticizer presents a tendency to increase plasticity allowing higher deformation, however, the tensile strength decreases [29]. It has also been discussed about the linearity in the tendency to enter the formulations in the preparation using the solvent-casting method to mechanical kneading, which in turn allows scaling up to conventional polymer processing methods [30].

3.7. Water vapor permeability (WVP)

The water vapor permeability (WVP) of the biodegradable films based is presented in Table 1, the starch control films (TPS100-CH0) presented a value of 26.20×10^{-11} $g.m^{-1}s^{-1}Pa^{-1}$. The amount of water vapor permeating through the material was decreased with the increase in the ratio of chitosan, being TPS25-CH75 ratio the one that reduces it the most, with a value of from 0.55×10^{-11} $g.m^{-1}s^{-1}Pa^{-1}$. The humidity of the material usually significantly modifies the barrier capacity of biodegradable materials. The higher the moisture content of the material, the barrier capacity is negatively affected, allowing more increased flow of gases. However, in the materials developed in this study, the film that absorbed the most moisture was the one that presented the best barrier to water vapor. The presence of water molecules and their interaction with the polar groups of the biopolymers through interchain hydrogen bonds progressively reduce the cohesive energy of the polymer, resulting in the plasticization of the matrix and increasing the diffusion coefficient. In chitosan, this behavior can be explained by higher hydrophilicity due to the presence of $-NH_3^+$ groups, amino and hydroxyl groups that represent binding sites for water molecules in the chitosan chain [31]. The hydrophobicity that chitosan generally presents causes a reduction in interactions with water molecules, reducing the permeation of water vapor [7]. The WVP values of the films developed in this study were significantly lower than those reported by other films made from different starches mixed with chitosan [15]. The materials developed in this study were a better barrier to moisture, which makes them a good alternative for use as food packaging.

4. Conclusions

Modified corn starch films mixed with different proportions of chitosan and plasticized with glycerol were developed and characterized by several techniques. Composite films were obtained with good workability and with good characteristics to be used as packaging material. Chitosan interacts effectively with starch, which was evidenced in the results obtained with FT-IR, XRD, DSC, TGA, and mechanical results where a strong interaction between both polymers was observed. Biodegradable films based on starch-chitosan mixtures exhibited an improved water vapor barrier compared to other starch-based materials. The formulation TPS25-CH75 blend was the one that obtained the lowest permeability to this gas, although the mechanical behavior was weaker than other mixtures.

The acetylation of starch is demonstrated by FT-IR and XRD where it is observed that the amylose and the amylopectin double helices were modified due to the substitution of OH groups by bulkier acetyl groups. Respecting the mechanical performance, the samples presented higher rigidity as the chitosan ratio increased, except for the TPS75-CH25 blend, which showed a ductility similar to the TPS100-CH0, but with better resistance. In addition, the thermal behavior in terms of the degradation temperature of this material was higher than the other formulations. These thermal transitions show miscibility between the components of the blends, with high degradation temperatures, making them susceptible and a good option for processing on a larger scale in plastic materials production equipment.

Author Contributions: Conceptualization, E.J.J.-R., and R.Y.A.-L.; methodology, A.F.-G., C.C.R.-V., and R.Y.A.-L.; formal analysis, C.C., A.F.-G. and R.Y.A.-L.; investigation, A.F.-G., E.J.J.-R. and R.Y.A.-L.; visualization, E.J.J.-R., and R.Y.A.-L.; supervision, E.J.J.-R. and R.Y.A.-L.; project administration, E.J.J.-R., and R.Y.A.-L.; funding acquisition, R.Y.A.-L., and C.C.; writing—original draft preparation, C.C., A.F.-G., E.J.J.-R., C.C.R.-V., and R.Y.A.-L.; writing—review and editing, A C.C., A.F.-G., E.J.J.-R., C.C.R.-V., and R.Y.A.-L. All authors have read and agreed to the published version of the manuscript.

Funding: This research was funded by Centro de Investigación en Química Aplicada (CIQA) under internal project 6610, and by Dirección General de Investigaciones (DGI) of Universidad Santiago de Cali under call no. 01-2021.

Data Availability Statement: The data presented in this study are available on request from the corresponding author.

Acknowledgments: Thanks to M.C. Blanca Huerta Martinez, M.C. Maria Guadalupe Mendez-Padilla, and M.C. Myrna Salinas Hernández for DRX, DSC, and TGA characterizations, respectively. Authors Fonseca-García (A.F.-G.) and Aguirre-Loredo (R.Y.A.-L.) thanks to CONACYT for their nominations as researchers assigned to CIQA. Carolina Caicedo (C.C.) acknowledge financial support from DGI of Universidad Santiago de Cali under project No. 939-621120-2148.

Conflicts of Interest: The authors declare no conflict of interest.

References

1. Katerinopoulou, K., et al., *Preparation and characterization of acetylated corn starch–(PVOH)/clay nanocomposite films.* Carbohydrate Polymers, 2014. **102**: p. 216-222.
2. Choo, K.W., M. Lin, and A. Mustapha, *Chitosan/acetylated starch composite films incorporated with essential oils: Physiochemical and antimicrobial properties.* Food Bioscience, 2021. **43**: p. 101287.
3. Colussi, R., et al., *Acetylated rice starches films with different levels of amylose: Mechanical, water vapor barrier, thermal, and biodegradability properties.* Food Chemistry, 2017. **221**: p. 1614-1620.
4. Calambas, H.L., et al., *Physical-Mechanical Behavior and Water-Barrier Properties of Biopolymers-Clay Nanocomposites.* Molecules, 2021. **26**(21): p. 6734.
5. Combrzyński, M., et al., *Physical Properties, Spectroscopic, Microscopic, X-ray, and Chemometric Analysis of Starch Films Enriched with Selected Functional Additives.* Materials, 2021. **14**(10): p. 2673.
6. Aranaz, I., et al., *Chitosan: An Overview of Its Properties and Applications.* Polymers, 2021. **13**(19): p. 3256.

7. Ferreira, R.R., et al., *Essential oils loaded-chitosan nanocapsules incorporation in biodegradable starch films: A strategy to improve fruits shelf life.* International Journal of Biological Macromolecules, 2021. **188**: p. 628-638.
8. Lipatova, I.M., et al., *Effect of composition and mechanoactivation on the properties of films based on starch and chitosans with high and low deacetylation.* Carbohydrate Polymers, 2020. **239**: p. 116245.
9. Fonseca-García, A., E.J. Jiménez-Regalado, and R.Y. Aguirre-Loredo, *Preparation of a novel biodegradable packaging film based on corn starch-chitosan and poloxamers.* Carbohydrate Polymers, 2021. **251**: p. 117009.
10. Wolf, W., W.E.L. Spiess, and G. Jung, *Standardization of Isotherm Measurements (Cost-Project 90 and 90 BIS)*, in *Properties of Water in Foods: in Relation to Quality and Stability*, D. Simatos and J.L. Multon, Editors. 1985, Springer Netherlands: Dordrecht. p. 661-679.
11. Aguirre-Loredo, R.Y., et al., *Effect of equilibrium moisture content on barrier, mechanical and thermal properties of chitosan films.* Food Chemistry, 2016. **196**: p. 560-566.
12. ASTM, *D882. Standard test method for tensile properties of thin plastic sheeting.* ASTM International, 2012.
13. ASTM, *E96. Standard Test Methods for Water Vapor Transmission of Materials.* ASTM International, 2002.
14. Ma, X. and J. Yu, *Formamide as the plasticizer for thermoplastic starch.* Journal of Applied Polymer Science, 2004. **93**(4): p. 1769-1773.
15. Meng, W., et al., *Effects of peanut shell and skin extracts on the antioxidant ability, physical and structure properties of starch-chitosan active packaging films.* International Journal of Biological Macromolecules, 2020. **152**: p. 137-146.
16. Ávila, A., et al., *Study of optimization of the synthesis and properties of biocomposite films based on grafted chitosan.* Journal of Food Engineering, 2012. **109**(4): p. 752-761.
17. Bernazzani, P., et al., *Evaluation of the phase composition of amylose by FTIR and isothermal immersion heats.* Polymer, 2008. **49**(19): p. 4150-4158.
18. Ma, Z., et al., *The retrogradation characteristics of pullulanase debranched field pea starch: Effects of storage time and temperature.* International journal of biological macromolecules, 2019. **134**: p. 984-992.
19. Fan, M., Q. Hu, and K. Shen, *Preparation and structure of chitosan soluble in wide pH range.* Carbohydrate Polymers, 2009. **78**(1): p. 66-71.
20. Diop, C.I.K., et al., *Effects of acetic acid/acetic anhydride ratios on the properties of corn starch acetates.* Food Chemistry, 2011. **126**(4): p. 1662-1669.
21. Singh, J., L. Kaur, and O.J. McCarthy, *Factors influencing the physico-chemical, morphological, thermal and rheological properties of some chemically modified starches for food applications—A review.* Food Hydrocolloids, 2007. **21**(1): p. 1-22.
22. Suyatma, N.E., et al., *Effects of Hydrophilic Plasticizers on Mechanical, Thermal, and Surface Properties of Chitosan Films.* Journal of Agricultural and Food Chemistry, 2005. **53**(10): p. 3950-3957.
23. Ramesh, N., et al., *Application of free-volume theory to self diffusion of solvents in polymers below the glass transition temperature: A review.* Journal of Polymer Science Part B: Polymer Physics, 2011. **49**(23): p. 1629-1644.
24. Gómez-Aldapa, C.A., et al., *Characterization of Functional Properties of Biodegradable Films Based on Starches from Different Botanical Sources.* Starch - Stärke, 2020. **72**(11-12): p. 1900282.
25. Qiao, C., et al., *Effect of hydration on water state, glass transition dynamics and crystalline structure in chitosan films.* Carbohydrate Polymers, 2019. **206**: p. 602-608.
26. Ferreira, M.L., et al., *The interaction between water vapor and chitosan II: Computational study.* Colloids and Surfaces A: Physicochemical and Engineering Aspects, 2008. **315**(1): p. 241-249.
27. Santacruz, S., C. Rivadeneira, and M. Castro, *Edible films based on starch and chitosan. Effect of starch source and concentration, plasticizer, surfactant's hydrophobic tail and mechanical treatment.* Food Hydrocolloids, 2015. **49**: p. 89-94.
28. Gao, C., et al., *Sustainable Chitosan-Dialdehyde Cellulose Nanocrystal Film.* Materials, 2021. **14**(19): p. 5851.
29. Tuhin, M.O., et al., *Modification of mechanical and thermal property of chitosan–starch blend films.* Radiation Physics and Chemistry, 2012. **81**(10): p. 1659-1668.
30. Epure, V., et al., *Structure and properties of glycerol-plasticized chitosan obtained by mechanical kneading.* Carbohydrate Polymers, 2011. **83**(2): p. 947-952.
31. Bourtoom, T. and M.S. Chinnan, *Preparation and properties of rice starch–chitosan blend biodegradable film.* LWT - Food Science and Technology, 2008. **41**(9): p. 1633-1641.